

Menno van der Veen
Ir. buro Vanderveen Zwolle The Netherlands

**Presented at
the 104th Convention
1998 May 16-19
Amsterdam**



AES

This preprint has been reproduced from the author's advance manuscript, without editing, corrections or consideration by the Review Board. The AES takes no responsibility for the contents.

Additional preprints may be obtained by sending request and remittance to the Audio Engineering Society, 60 East 42nd St., New York, New York 10165-2520, USA.

All rights reserved. Reproduction of this preprint, or any portion thereof, is not permitted without direct permission from the Journal of the Audio Engineering Society.

AN AUDIO ENGINEERING SOCIETY PREPRINT

Modelling Power Tubes and their Interaction with Output Transformers

MENNO VAN DER VEEN, AES member

ir. buro Vanderveen, The Netherlands
fax: 31-38-4533-178, e-mail: mennovdv@noord.bart.nl

New pentode power tube and output transformer models are derived and tested offering detailed information about dynamic and static behaviour of tube push-pull audio amplifiers. A 'Super Pentode' tube amplifier circuit topology and toroidal 'specialist' output transformers are introduced.

0 INTRODUCTION

In a previous preprint (1) an equivalent model for toroidal output transformers was developed for audio push-pull tube amplifiers (figure 0-1). In that model the power tubes which drive the output transformer behave like alternating voltage sources with their plate resistances in series (figure 0-2).

This model produces accurate results in the frequency domain; however it does not indicate the available output power, optimal primary impedance of the output transformer, damping factor, amplification, distortion and output power dependent changes in these quantities. To learn more about these factors the model needs extension and this is discussed in the present paper.

First, in section 1, the simple model of figure 0-2 is replaced by a new model based on an extension of the Child-Langmuir equation. It delivers detailed information about voltages on and currents through every element of the tube as function of the control grid or the anode voltages. The results of this model are compared with measured data in section 2.

Secondly, it was realised that not all tube push-pull audio amplifiers are in the standard pentode configuration. Ultra-Linear, Triode, various degrees of Cathode Feedback as well as Unity Coupled push-pull configurations are used worldwide. Therefore, in section 3 a new generalised push-pull output transformer coupling model is developed in which any possible (sensible) push-pull amplifier configuration can be described.

Combining the new power tube equivalent model with the generalised output transformer coupling model offers the possibility to calculate the above mentioned quantities. To compare theory and practice, eight test amplifiers were built with new toroidal 'specialist' output transformers. Results of the maximum output power and the damping factor are shown in section 4. A newly developed, so called ' Super Pentode ' configuration is introduced in section 5.

1 PENTODE TUBE EQUIVALENT MODEL

Figure 1-1 shows a pentode tube and defines the voltages on and currents through the cathode, grids and anode. The standard equation (Child-Langmuir) for the cathode current is given by formula 1.1

For the distribution of the cathode current into the anode and screen grid currents several models are proposed in (2), (3), (4) and (5).

The newly developed model is only ment for pentode tubes. It introduces a current distribution function $\alpha(V_{ak}, V_{g2k})$ based on the voltage ratio (V_{ak} / V_{g2k}) . Its behaviour is shown in figure 1-2 for $1 < n < 10$ and for $0 < (V_{ak} / V_{g2k}) < 3$.

$$I_k = K \cdot [V_{g1k} + D_{g2} \cdot V_{g2k} + D_a \cdot V_{ak}]^{1.5} \quad (1.1)$$

$$\frac{I_a}{I_k} = \alpha(V_{ak}, V_{g2k}) = \alpha_0 \cdot \left[\frac{2}{\pi} \cdot \arctan\left(\frac{V_{ak}}{V_{g2k}}\right) \right]^{\frac{1}{n}} \quad (1.2)$$

$$I_{g2} = I_k - I_a \quad (1.3)$$

In this model 5 parameters [n , α_0 , K , D_a , D_{g2}] are needed to characterise a pentode power tube.

2 CONVERTING TUBE PARAMETERS

Tube handbooks specify power tubes by means of the transconductance (g_m or S), the plate resistance (r_i or r_a or r_p) and the amplification factors μ and μ_{g1g2} in a set-up point characterised by I_a , I_{g2} , V_{ak} , V_{g2k} and V_{g1k} . These specifications can be converted into the five [n , α_0 , K , D_a , D_{g2}] parameter values. Some extra formulas are needed for this conversion. See formulas 2.1, 2.2 and 2.3.

$$S = \frac{\partial I_a}{\partial V_{g1k}} = \frac{3}{2} \cdot [K \cdot \alpha(V_{ak}, V_{g2k})]^{\frac{3}{2}} \cdot I_a^{\frac{1}{3}} \quad (2.1)$$

$$r_i = \left[\frac{\partial I_a}{\partial V_{ak}} \right]^{-1} = \left[D_a \cdot S + \frac{I_a}{\alpha(V_{ak}, V_{g2k})} \cdot \frac{\partial \alpha(V_{ak}, V_{g2k})}{\partial V_{ak}} \right]^{-1} \quad (2.2)$$

$$\mu = \frac{\partial V_{ak}}{\partial V_{g1k}} = \left[D_a + \frac{I_a}{\alpha(V_{ak}, V_{g2k})} \cdot S \cdot \frac{\partial \alpha(V_{ak}, V_{g2k})}{\partial V_{ak}} \right]^{-1} \quad (2.3)$$

$$\frac{\partial \alpha(V_{ak}, V_{g2k})}{\partial V_{ak}} = \alpha(V_{ak}, V_{g2k}) \cdot \frac{1}{\arctan\left(\frac{V_{ak}}{V_{g2k}}\right)} \cdot \frac{1}{1 + \left(\frac{V_{ak}}{V_{g2k}}\right)^2} \cdot \frac{1}{V_{g2k}} \cdot \frac{1}{n} \quad (2.4)$$

As an example the conversion of the information from a tube handbook into the five parameter set is shown. A tube handbook (6) delivers the following information of an EL34 pentode: $S = 12.5$ [mA/V] and $r_i = 17$ [kΩ] at $I_a = 100$ [mA], $I_{g2} = 15$ [mA], $V_{ak} = 250$ [V], $V_{g2k} = 265$ [V] and $V_{g1k} = -13.5$ [V].

We start by giving n a value between 1 and 10. For instance $n = 5$. Formula 1.2 now gives $\alpha_o = 1.006$ []; formula 2.1: $K = 2.766 \cdot 10^{-3}$ [A.V^{-1.5}]; formula 2.4 delivers $\partial \alpha(V_{ak}, V_{g2k}) / \partial V_{ak}$. D_a can be calculated now with the value of r_i and formula 2.2: $D_a = 0.482 \cdot 10^{-3}$ []. Finally with formula 1.1: $D_{g2} = 95.77 \cdot 10^{-3}$ [].

2.1 Results

Figures 2-1, 2-2 and 2-3 show the calculated characteristics of the EL34 tube for $n = 1, 5$ and 10 . Figure 2-4 gives the measured data of an EL34 tube. Comparison with figure 2-2 shows that for $n = 5$ there is good agreement.

3 GENERALISED COUPLING MODEL

In push-pull tube amplifiers with the power tubes in the pentode or triode mode, the coupling between the tubes and the output transformer is adequately described by the drawing of a loadline in the I_a - V_{ak} - V_{g1k} -characteristics of the tubes.

However, the situation becomes more complex when the screen grids are connected to taps on the primary winding and when cathode feedback is applied.

A new coupling model is developed to describe such a situation. Figure 3-1 shows the general amplifier schematics. The cathodes are connected to a winding with N_k turns, the screen grids are connected to N_{sch} turns and the anodes to N_p turns. Formulas 3.1 and 3.2 define the turn ratios of these windings.

$$X = \frac{N_{sch}}{N_p} \quad X > 0 \text{ for negative feedback} \quad (3.1)$$

$$\Gamma = \frac{N_k}{N_p} \quad \Gamma > 0 \text{ for negative feedback} \quad (3.2)$$

The tubes are supplied with power (V_{g20} and V_{a0}). The negative voltage supply V_{g10} defines the tubes quiescent currents. The alternating input voltage ΔV is connected in opposite phase to the control grids through capacitors.

Figure 3-2 shows the voltages at the upper tube $j=1$. Suppose that the anode is at a momentary voltage of V_{a1} and the input voltage at ΔV . The momentary voltages at all the tube elements referred to their cathode are given by formula 3.3.

$$\begin{aligned} V_{g1k-1} &= V_{g10} + \Delta V + \Gamma \cdot (V_{a1} - V_{a0}) \\ V_{g2k-1} &= V_{g20} + (X + \Gamma) \cdot (V_{a1} - V_{a0}) \\ V_{ak-1} &= V_{a1} + \Gamma \cdot (V_{a1} - V_{a0}) \end{aligned} \quad (3.3)$$

A same formula set can be derived for the lower tube $j = 2$. With formulas 1.1, 1.2 and 1.3 all the momentary currents I_{a-j} , I_{g2-j} and I_{k-j} in the tubes $j = 1$ and 2 can be calculated now as a function of ΔV and V_{a1} .

With the use of $\alpha(V_{ak-j}, V_{g2k-j})$, abbreviated to α_j , all these currents can be expressed in I_{a-j} . Combined with the turn ratios X and Γ , it can easily be shown that each tube effectively acts as one current source I_{eff-j} driving $\frac{1}{2}N_p$ turns.

$$I_{eff-j} = I_{a-j} \cdot \left(1 + \frac{X \cdot (1 - \alpha_j)}{\alpha_j} + \frac{\Gamma}{\alpha_j} \right) \quad (3.4)$$

$I_{\text{eff-1}}$ flows in the opposite direction from $I_{\text{eff-2}}$ through its half of the primary winding. Formula 3.5 gives the resulting current δI_{eff} of both tubes combined.

$$\delta I_{\text{eff}} = I_{\text{eff-1}} - I_{\text{eff-2}} \quad (3.5)$$

The whole circuit of power tubes plus transformer can be replaced now by one single current source δI_{eff} driving $\frac{1}{2}N_p$ turns. Formula 3.6 gives the internal resistance $r_{i\text{-eff}}$ of this current source $\{ \partial V_{a1} = - \partial V_{a2} \}$:

$$r_{i\text{-eff}} = \left[\frac{\partial}{\partial V_{a1}} \delta I_{\text{eff}} \right]^{-1} = \left[\frac{\partial I_{\text{eff-1}}}{\partial V_{a1}} + \frac{\partial I_{\text{eff-2}}}{\partial V_{a2}} \right]^{-1} = \left[\frac{1}{r_{i-1}} + \frac{1}{r_{i-2}} \right]^{-1} \quad (3.6)$$

The new equivalent circuit of the power tubes plus the output transformer is shown in figure 3.3. Both δI_{eff} and $r_{i\text{-eff}}$ are functions of V_{a1} and ΔV .

By Ohms law the ratio of V_{a1} and δI_{eff} equals $\frac{1}{4}Z_{aa}$ in which Z_{aa} is the impedance of the primary anode to anode winding (N_p turns). This means, combined with the above given relations, that all the momentary currents and voltages are only functions of ΔV or V_{a1} . This completes the definition of the coupling model.

4 APPLICATIONS IN EIGHT AMPLIFIERS

To test the validity of the tube and coupling models, eight test amplifiers were built. Various $\{X, \Gamma\}$ combinations were tested by using different taps on the toroidal push-pull output transformer VDV-2100-CFB/H ((7), (8)) with $N_p / N_s = 20$, $X = \{-1, -0.33, 0, 0.33, 1\}$ and $\Gamma = \{-0.1, 0, 0.1\}$. Figure 4-1 shows the schematics of the test amplifiers and the $\{X, \Gamma\}$ combinations selected.

The EL34 tubes used in these experiments were tested in detail resulting in the 'EL34-Old' parameter set given in table 4-2. These parameters deviate from the chapter 2 'EL34-New' parameters because the tubes previously have been used for more than 3000 burning hours. Their smaller K-value indicates the aging.

The anode and screengrid power supplies V_{a0} and V_{g20} were set at 450 V while the quiescent anode current per tube equaled 45 mA. Calculation of V_{g10} with formulas 1.1 and 1.2 results in $V_{g10} = -36.2$ V while $V_{g10} = -37$ V was measured.

The impedance of the load connected to N_s was 8 Ω . The total primary impedance combined with the resistances of the primary and secondary windings gives a total effective primary impedance of $Z_{aa} = 3300 \Omega$.

Two test results will be studied in detail now: the maximum output power P_{\max} and the effective internal resistance $r_{i\text{-eff}}$ at small output powers.

4.1 Calculation of P_{\max}

The maximum output power situation (at clipping) is reached when in tube $j=1$ $V_{g1k-1} = 0$ V while $V_{g1k-2} = 2V_{g10}$ and visa versa. Under this condition formula 3.3 changes into $V_{g1k-1} = 0$ while V_{g2k-1} and V_{ak-1} remain unchanged.

All the currents can be calculated now as a function of V_{a1} . Taking test amplifier 5 with $\{X, \Gamma\} = \{-0.33, 0.1\}$ as an example, figure 4-3 shows the resulting δI_{eff} as a function of V_{a1} .

In figure 4-3 the loadline of an arbitrary output transformer (with slope $1/4Z_{aa}$) is drawn. At the crossing point of δI_{eff} and this loadline both V_{a1} and δI_{eff} are known. Then P_{\max} is given by $1/2(V_{a0} - V_{a1})\delta I_{\text{eff}}$ while Z_{aa} equals $4(V_{a0} - V_{a1}) / \delta I_{\text{eff}}$.

This means that P_{\max} and Z_{aa} are interrelated through V_{a1} . By changing V_{a1} from 0 to V_{a0} their interdependance can be calculated. Figure 4-4 shows the result for test amplifier 5. The maximum output power is reached for Z_{aa} close to 3 k Ω .

Using the same calculation procedure the maximum output power of each test amplifier can be calculated now with the known value of $Z_{aa} = 3.3$ k Ω . The insertion loss created by the winding resistances of the output transformer equals 3 %. The calculated P_{\max} values shown are corrected for this loss. See table 4-5.

4.2 Maximum Power results

With 1 kHz sine wave input voltages the test amplifiers were driven upto clipping. P_{\max} was measured with an oscilloscope connected over the 8 Ω secondary load. Table 4-5 gives the measurement results and comparison with the calculated values shows the agreement.

4.3 Calculation of $r_{i\text{-eff}}$

With formula 3.6 the internal resistances r_{i-j} and $r_{i\text{-eff}}$ can be calculated as a function of V_{a1} . As an example figure 4-6 shows the calculated internal resistances of test amplifier 5 as a function of V_{a1} . It is clearly visible that these resistances are not constant but change with the momentary value of V_{a1} . Therefore the calculations and tests were performed for V_{a1} staying very close to V_{a0} , meaning that the measurements were done at very small output levels (10 mW in 8 Ω).

4.4 Internal Resistance results

When the 'EL34-Old' parameter set of table 4-2 was used to calculate the effective internal resistances of the eight test amplifiers, a deviation upto a factor 2 with the measured values was noticed. Therefore the five parameter set was remeasured in the close environment of the quiescent condition (V_{a1} almost equal to V_{a0}), resulting in a 'small-signal' five parameter set of the EL34-Old tubes. See for details table 4-2.

With this 'small-signal' parameter set the $r_{i\text{-eff}}$ values were recalculated and compared to the measured values. See table 4-7 for the agreement between measurement and calculations.

4.5 Further Results

In further tests the amplification and distortion behaviour (by means of Lissajous figures) and frequency range were researched, showing agreement between calculations and measurements. Again the validity of the coupling model was found and the sensitivity of the tube modelling to large or small signal conditions was noticed.

5 INTRODUCING THE 'SUPER PENTODE' CONFIGURATION

The work presented in the previous chapters has shown that the maximum output power P_{max} and the effective internal resistance $r_{i\text{-eff}}$ of a push-pull tube amplifier are functions of the parameters given in formula 5.1 and 5.2.

$$P_{\text{max}} = f(Z_{aa}, V_{a0}, V_{g20}, X, \Gamma) \quad (5.1)$$

$$r_{i\text{-eff}} = f(Z_{aa}, V_{a0}, V_{g20}, V_{g10}, X, \Gamma) \quad (5.2)$$

The aim of this research was to develop the fundamental theory for the design of new wide bandwidth toroidal output transformers for push-pull tube amplifiers (the 'specialist range': see (7) and (8)). This meant that standard conditions should be defined for which those new transformers would be best suited. The choice was made to optimize for $V_{a0} = V_{g20} = 450 \text{ V}$.

This research has shown that P_{\max} would be maximum for $Z_{aa} = 3 \text{ k}\Omega$. Therefore transformers with Z_{aa} ranging from $2 \text{ k}\Omega$ to $4 \text{ k}\Omega$ were developed. The theory shows that only $r_{i\text{-off}}$ is sensitive to the quiescent current I_{a0} which can be defined freely through V_{g10} by the user.

Under these conditions both P_{\max} and $r_{i\text{-off}}$ are only determined by X and Γ . The next goals were: develop an amplifier configuration with these new transformers with a larger output power than the standard push-pull pentode amplifier and give that amplifier a damping factor close to the damping factor of triode amplifiers.

The calculations and measurements showed that both conditions could be met in the Super Pentode[®] configuration with $X = -0.33$ and $\Gamma = 0.1$ or combined values nearby.

An other way of dealing with the Super Pentode: applying only cathode feedback ($\Gamma > 0$) has the disadvantage that the (not constant) screen grid current flows through the cathode winding and consequently creates more or less unwanted distortion. By choosing just that amount of positive screen grid feedback ($x < 0$), combined with $\Gamma > 0$, the situation can be created that the effective contribution of the screen grid current to the magnetic field in the core is cancelled out. See figure 5-1 showing the different currents in the Super Pentode amplifier, where δI_{off} and I_{a-1} almost coincide.

6 CONCLUSIONS

In this preprint two new models are introduced. The output transformer coupling model is able to predict push-pull tube amplifier behaviour when the fundamental parameters of the push-pull power tubes and the output transformer are known. It gives accurate results of the maximum output power and the damping factor and is able to predict the frequency range, the power bandwidth and the distortion behaviour. The pentode power tube model uses a new current distribution function α_j , combined with the well known Child-Langmuir equation, resulting in a five parameter set, characterising the tubes applied.

Tests of both models in eight tube amplifiers showed the validity of the output transformer coupling model. It has been noticed that the working region of the new tube equivalent model has to be split into two areas (small and large signal) in order to deliver reliable results. This is in agreement with remarks made in (5) about the limited validity of tube modelling with few parameters. Therefore this tube equivalent model is subject to further improvement.

As a result of the new models the Super Pentode[®] push-pull amplifier configuration was invented and new Specialist Output Transformers could be developed.

7 ACKNOWLEDGMENT

The author wishes to thank Amplimo and Plitron for their support and Dr. Ir. M. Boone, Delft University of Technology, Laboratory of Seismics and Acoustics, the Netherlands, for his valuable contribution.

8 REFERENCES

- 1) **Menno van der Veen**: "Theory and Practice of Wide Bandwidth Toroidal Output Transformers"; AES preprint 3887 (G-2); 97th AES-Convention; 1994; San Francisco.
- 2) **Scott Reynolds**: "Vacuum-Tube Models for PSPICE Simulations"; Glass Audio; Volume 5/4; 1993.
- 3) **W. Marshall Leach, Jr.**: "SPICE Models for Vacuum-Tube Amplifiers"; JAES; Volume 43/3; 1995; March.
- 4) **Norman Koren**: "Improved Vacuum-Tube Models for SPICE Simulations"; Glass Audio; Volume 8/5; 1996.
- 5) **"Letters to the Editor"**; JAES; Volume 45/6; 1997; June.
- 6) **De Muiderkring**: "Tube & Transistor Handbook"; Volume 1; November 1964
- 7) **Menno van der Veen**: "Specialist Ringkern Uitgangstransformatoren; de Super-Pentode-Schakeling ©"; Amplimo b.v. Delden; www.amplimo.nl
- 8) **Menno van der Veen**: "Lab Report Specialist Range Toroidal Output Transformers"; Plitron Manufacturing Inc. Toronto; www.plitron.com

Super Pentode ©: An amplifier is in the Super Pentode configuration for those $\{x, \Gamma\}$ combinations where $X < 0$ and $\Gamma > 0$, excluding the $\{X, \Gamma = -1, 1\}$ combination, which is owned by McIntosh. Name and principle are registered by the author and are subject to European Union and International Copyright Laws. Licensing Enquires for reproduction of and manufacture for trade sale should be directed to Menno van der Veen.

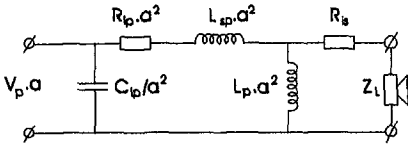


Figure 0-1: Equivalent Circuit Output Transformer

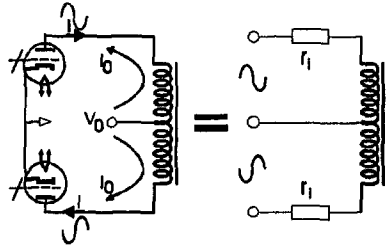


Figure 0-2: Basic Equivalent Circuit Power Tubes

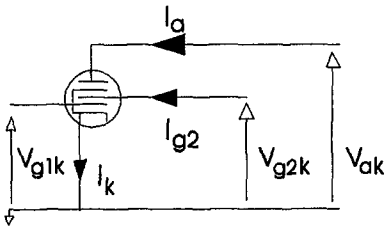


Figure 1-1: Currents and Voltages at a Pentode

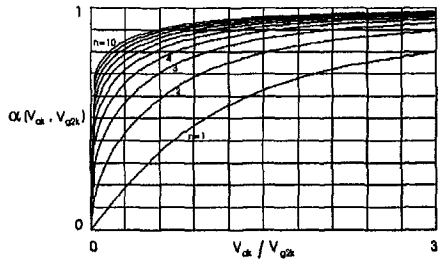


Figure 1-2: Current Distribution Function

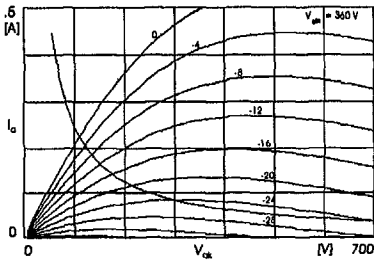


Figure 2-1: EL34 Characteristics for $n = 1$

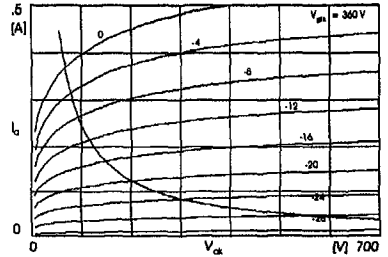


Figure 2-2: EL34 Characteristics for $n = 5$

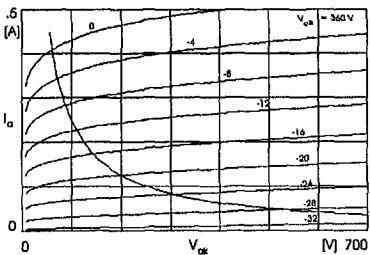


Figure 2-3: EL34 Characteristics for $n = 10$

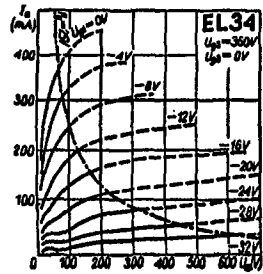


Figure 2-4: EL34 Characteristics measured

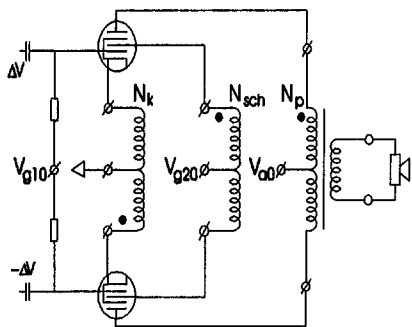


Figure 3-1: Transformer Coupling Model Configuration

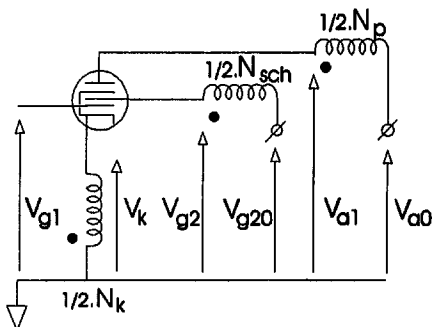


Figure 3-2: Voltages by tube $j = 1$

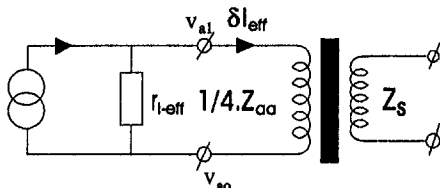


Figure 3-3: Current Source Equivalent Model

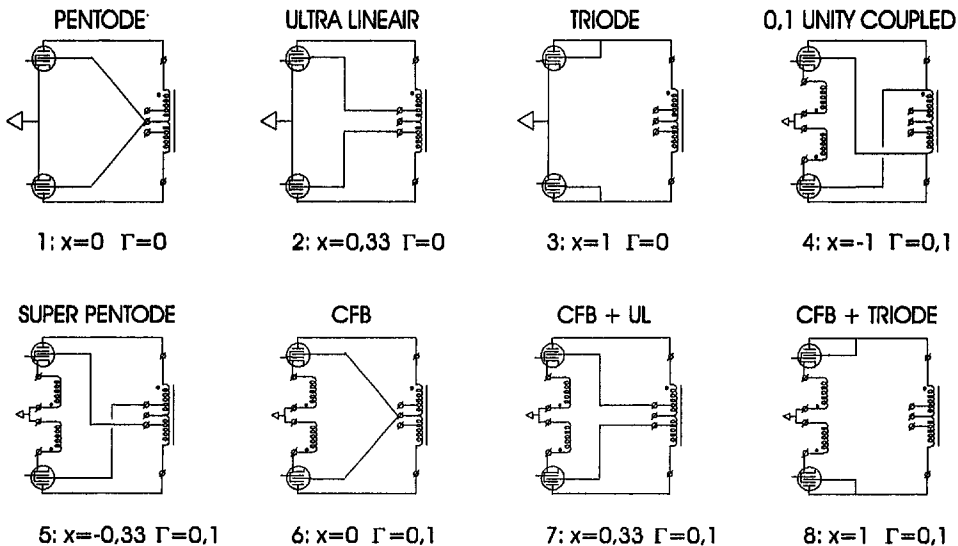


Figure 4-1: Eight Test Amplifier Configurations

FIG.	TUBE + remarks	n	α_o	K	D_1	D_2
2-1	EL34; see chapter 2	1	1.806	$2.766 \cdot 10^{-3}$	$-16.41 \cdot 10^{-3}$	$111.7 \cdot 10^{-3}$
2-2	EL34; see chapter 2	5	1.006	$2.766 \cdot 10^{-3}$	$0.482 \cdot 10^{-3}$	$95.77 \cdot 10^{-3}$
2-3	EL34; see chapter 2	10	0.936	$2.766 \cdot 10^{-3}$	$2.594 \cdot 10^{-3}$	$93.78 \cdot 10^{-3}$
4-5	EL34-OLD; P_{max} -calc.	5	0.992	$2.188 \cdot 10^{-3}$	$2.343 \cdot 10^{-3}$	$96.5 \cdot 10^{-3}$
4-7	EL34-OLD; r_i -calc.	5	0.992	$0.898 \cdot 10^{-3}$	$4.241 \cdot 10^{-3}$	$109.3 \cdot 10^{-3}$
Unit	-	-	-	[A.V ^{-1.5}]	-	-

Table 4-2: tube 5-parameter-sets

amplifier \rightarrow	1	2	3	4	5	6	7	8	Unit
P_{max} measured	74	55	27	/	80	63	49	27	W
P_{max} calculated	74	55	27	/	78	72	53	26	W

Table 4-5: Measured and Calculated Maximum Output Power

amplifier \rightarrow	1	2	3	4	5	6	7	8	Unit
r_{i-eff} measured	15.7	2.39	0.84	/	1.23	0.83	0.61	0.40	k Ω
r_{i-eff} calculated	15.7	2.541	0.844	/	1.239	0.842	0.622	0.387	k Ω

Table 4-7: Measured and Calculated Effective Internal Resistance

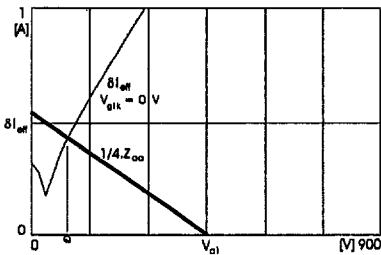


Figure 4-3: Calculation Method of Pmax

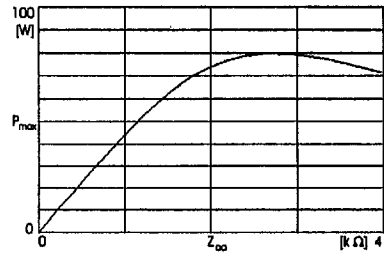


Figure 4-4: Pmax as a function of Zaa

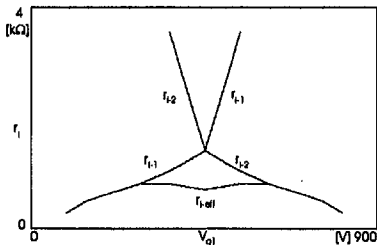


Figure 4-6: Internal Resistances of both tubes and the Total Effective Internal Resistance

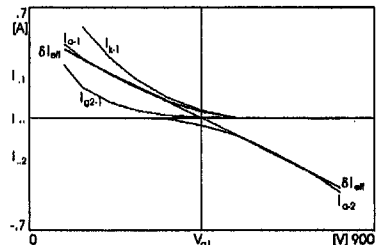


Figure 5-1: Currents in Tubes $j = 1 \& 2$ and the Effective Difference Current